JPE 18-6-11

https://doi.org/10.6113/JPE.2018.18.6.1720
ISSN(Print): 1598-2092 / ISSN(Online): 2093-4718

Novel Soft Starting Algorithm of Single Phase Induction Motors by Using PWM Inverter

Hae-Jin Kim*, Seon-Hwan Hwang**, and Jang-Mok Kim†

*CAC Engineering Department, LG Electronics, Changwon, Korea
**Department of Electrical Engineering, Kyungnam University, Changwon, Korea
†Department of Electrical Engineering, Pusan National University, Busan, Korea

Abstract

This paper proposes a novel soft starting algorithm by using PWM inverter technique to control an amplitude of the motor starting current at a single-phase induction motor (SPIM). Traditional SPIM starting methods such as a Split-Phase, Capacitor-Start, Permanent-Split Capacitor (PSC), Capacitor-Start Capacitor-Run (CSCR), basically cannot control the magnitude of starting current due to the fixed system structures. Therefore, in this paper, a soft starting algorithm based on a proportional resonant (PR) control with a variable and constant frequency is proposed to reduce the inrush current and starting up time. In addition, a transition algorithm for operation modes is devised to generate a constant voltage and constant frequency (CVCF). The validity and effectiveness of the proposed soft starting method and transition algorithm are verified through experimental results.

Key words: Capacitor-Start Capacitor-Run, Operation mode transition, PR (Proportional Resonant) current controller, Soft starting algorithm, SPIM

I. INTRODUCTION

Single-phase induction motors (SPIMs) are robust, easy to maintain and their cost is low. So SPIMs are widely used in many industrials and home appliances such as washing machines, dishwashers, refrigerators, air-conditioners, vacuum cleaners, pumps, compressors, etc. However, unlike a three-phase induction motor, the SPIMs cannot produce their own starting torque. Instead, the magnetic field generated by a single phase remains stationary in position and pulsates with time. Because there is no rotating magnetic field, a SPIM cannot run by itself without additional equipment.

As a result, traditional methods to start a SPIM include Split-Phase, Capacitor-Start, Permanent-Split Capacitor (PSC), Capacitor-Start Capacitor-Run (CSCR), and Shaded-Pole (SP) [1], [2]. However, when a SPIM is started by the direct starting methods of the fixed system structures, the motor starting current can be around 500~700% of the rated motor current, which can cause an over current to electrical systems and a torque surge to mechanical systems. There have been many different studies to reduce starting current. Firstly, an auto-transformer and a tapped winding arrangement are used to reduce the voltage amplitude which is supplied to a SPIM for limiting starting current [3]. But, when considering the size, weight and costs of the transformer, this method may not be favorable. Secondly phase control techniques are effective and low-cost methods for reducing large starting currents by using thyristor-based voltage control [4]. However, these methods result in discontinuous input current waveforms which contain odd and even harmonics as well as sub-harmonics of the supply frequency which exceed harmonic limit standards.

Therefore, nowadays Pulse Width Modulation (PWM) inverter methods have become powerful as an alternative because these techniques can overcome the problems associated with the conventional thyristor-based voltage control. Various PWM converter topologies such as a dc-link converter and an ac-ac converter have been investigated [5], [6]. The PWM operation at high chopping frequencies will result in harmonics appearing at higher frequencies where they can be easily eliminated by a small sized filter [7].

Manuscript received Apr. 2, 2018; accepted Aug. 9, 2018
Recommended for publication by Associate Editor Wook-Jin Lee.
†Corresponding Author: jmok@pusan.ac.kr
Tel: +82-51-510-2366, Fax: +82-51-513-0212, Pusan Nat'l University
*CAC Engineering Dept., LG Electronics, Korea
**Dept. of Electrical Eng., Kyungnam University, Korea

PI current controller is the most powerful among controllers in PWM inverters. The synchronous frame PI current regulator of a PWM inverter has good performance for reducing starting current [8]. But this method has a long starting time due to calculation of the transformation between stationary reference frame and synchronous reference frame, and the 90° phase delay to get the q-axis variable in a single phase system.

As the starting time is longer, it has a negative effect on some systems, such as compressor applications.

In this paper, a novel soft starting scheme is proposed by using Proportional Resonant (PR) current controller. The PR controller provides an infinite gain at the selected frequency (resonant frequency) and a zero phase shift. PR controller has a similar performance as PI regulator to reduce starting current. Once again, since a PR regulator does not require a reference frame transformation and need to obtain q-axis variable, it can reduce starting up time. The proposed PR current controller operates on variable and constant frequency modes.

The SPIM which is used for ultra-low temperature freezer, runs at a constant speed of 50 [Hz] or 60 [Hz] after starting operation. If both main and auxiliary windings stator currents are measured and controllable, sensorless control methods can be applied [9], [10]. However, in the 2 legs inverter case of SPIMs, these windings cannot be measured and controlled separately. Therefore, it is structurally not possible to control speed by sensorless methods.

Since sensorless speed control is not available after start-up, the transition algorithm is designed to control a constant voltage and constant frequency at the steady state. The usefulness and effectiveness of the proposed algorithms is verified through several experiments and performance comparison with voltage control techniques that are widely used, such as variable voltage constant frequency (VVCF) and variable voltage variable frequency (VVVF).

II. Configuration of a CSCR-PTC for a SPIM

Fig. 1 shows the configuration of a CSCR-PTC for starting a SPIM in order to control the compressor of an ultra-low temperature freezer. The motor is composed of two stator windings, which are a main winding and an auxiliary winding with a PTC starter.

As shown in Fig. 2, a CSCR builds up not only the starting torque of SPIM by starting and running capacitor at start-up time but also improves the performance of a SPIM by running capacitor at steady state period [1]. Current path of the PTC is disconnected from the circuit when the current reaches a certain amount and the resistance gets large during the start up.

However, the starting current of the CSCR method can be around 500 ~ 700% of the motor full-load current. This large current happens during start up, normally within 1 second. It

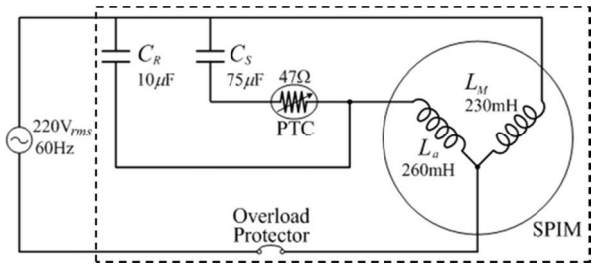

Fig. 1. Configuration of a SPIM (CSCR-PTC).

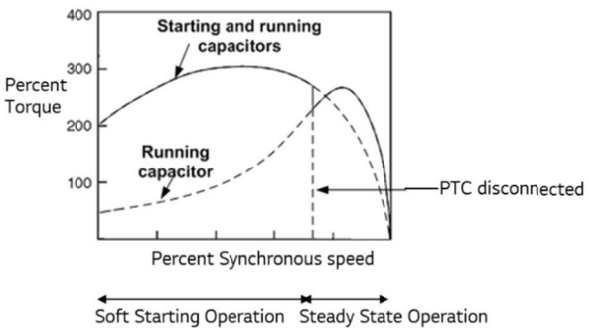

Fig. 2. Speed-torque characteristic curve of a CSCR-PTC.

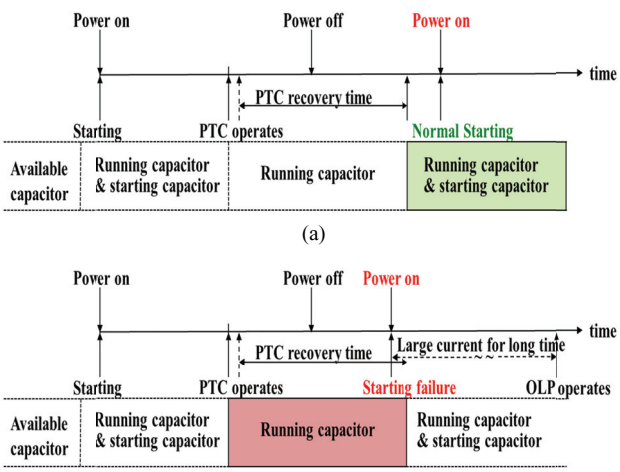

Fig. 3. Starting operations of a CSCR-PTC: (a) Normal starting (Power on after PTC recovery time); (b) Starting failure and OLP operation (Power on before PTC recovery time).

can result in abnormal operation to electrical systems and mechanical systems.

Fig. 3 shows starting operation of a CSCR-PTC. The starting operation is normally successful when power-on occurs after the PTC recovery time. However, as shown in Fig. 3(b), the starting operation will be fail when trying to start the system before the recovery of PTC because only the running capacitor is available at this time. In this case, the Over Load Protector (OLP) operates to cut off the large current which has been maintained for long time, normally 10 ~ 20 seconds, and it can cause electrical and mechanical damage to the system. Therefore, the inrush current of a

TABLE I
COMPARISONS OF THE SWITCH AND CURRENT SENSOR NUMBERS ACCORDING TO THE INVERTER TOPOLOGIES

Contents	Constant speed operation	Sensorless speed control
Inverter system	2 legs inverter	3 legs inverter
Number of switches	4	6
Number of current sensors	1	2
Separate current control (main, aux.)	Not available	Available

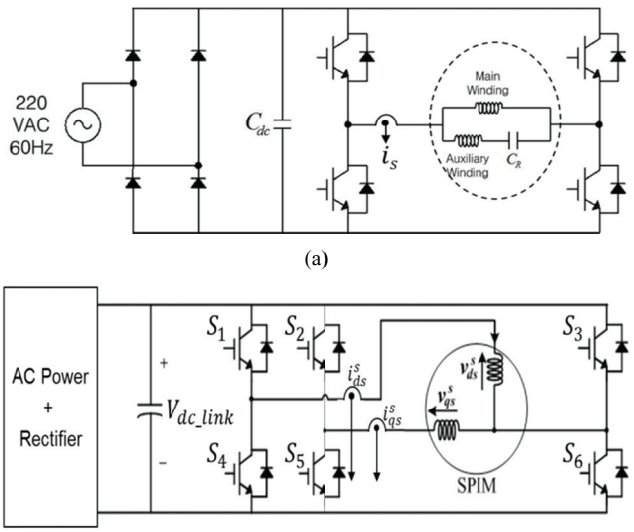

Fig. 4. Single-phase PWM inverters for compressor with a SPIM: (a) 2 legs inverter of SPIM; (b) 3 legs inverter of SPIM.

SPIM must be improved.

Ones more, as previously mentioned, if the currents of main winding and auxiliary winding can be measured, sensorless control is possible. However, it needs more current sensors and switching devices due to the three-legs inverter as described at Table I and Fig. 4. This leads to increases in the control complexity and costs.

The system used in this paper uses constant speed operation to avoid increasing the control complexity and costs. As a result, it cannot continuously use a current controller after the starting operation since sensorless control is not available.

Therefore, a mode transition algorithm is devised to operate a SPIM at a constant voltage and constant frequency in the steady state operation region.

III. PROPOSED CONTROL STRATEGIES FOR SOFT STARTING AND OPERATION MODE TRANSITION

A. Soft Starting Control

A single-phase full-bridge PWM inverter is shown in Fig. 4. A full-bridge diode rectifier and a full-bridge inverter are used with a dc link capacitor which supplies the reactive power to the motor. A synchronous frame PI current controller has good performance to reduce the starting current. However, it has a complex calculation due to synchronous frame controller related problems in SPIMs, which result in increased starting time.

In addition, oil ring operation is important in terms of the reliability of a compressor. The oil ring operates when a motor starts to rotate. Normally, this occurs before compressor reaches 60 Hz. If oil ring operates late, this leads to mechanical wear which can damage the compressor. The starting time should be reduced as much as possible to start the oil ring operation. In this paper, a soft starting algorithm using a PR controller is proposed to reduce the starting time of SPIMs.

The PR controller provides an infinite gain at the resonant frequency with a zero-phase shift. An ideal PR controller can be expressed as:

$$G_{PR\_ideal}(s) = K_{pn} + \sum_n \frac{K_{in}s}{s^2 + (n\omega_o)^2} \quad (1)$$

where K_{pn} is the proportional gain, K_{in} is the resonant gain, n is the harmonic number, and ω_0 is the resonant angular frequency. Because of the infinite gain, it provides zero steady state error which is the same error as a synchronous frame PI current controller with a phase angular rotating at the resonant frequency [11].

However, if controlling frequency is slightly different from resonant frequency, the performance degrades considerably in an ideal PR controller. To compensate for the disadvantage of an ideal PR controller, a practical PR controller is commonly used by modifying the gain and bandwidth. The transfer function of a practical PR controller can be defined by Equ. (2).

$$G_{PR\_prac}(s) = K_{pn} + \frac{2K_{in}\omega_c s}{s^2 + 2\omega_c s + \omega_o^2} \quad (2)$$

where ω_c is the bandwidth at -3dB cutoff frequency of the controller and the gain of the controller at ω_0 - ω_c and ω_0 + ω_c is $K_{in}/\sqrt{2}$ [12].

Fig. 5 shows a bode plot of the practical PR controller. The parameters used are: proportional gain K_{pn} = 0.2, resonant gain K_{in} = 1, and bandwidth at cutoff frequency of ω_c = 10. The magnitude and phase of the systems depend on variations of the parameters. K_{pn} determines the dynamics of the controller while K_{in} determines gain at a selected frequency and controls the bandwidth [13]. Finally, a control block diagram of the proposed soft starting algorithm is shown in Fig. 6.

While providing equivalent performance as a synchronous PI current controller, the PR current controller in the stationary frame does not have synchronous frame controller related problems such as a reference frame transformation and 90° phase delay to get the q-axis variable in a single phase system [14]. Since this topology has simpler calculations than

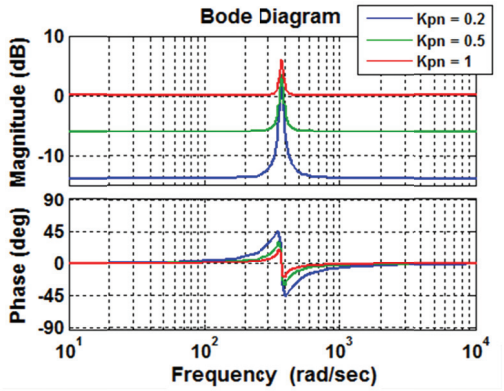

(a)

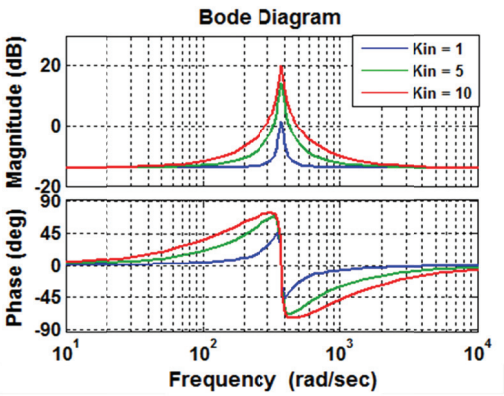

(b)

Fig. 5. Bode plots of a practical PR controller according to parameter variations: (a) K_{pn}; (b) K_{in}.

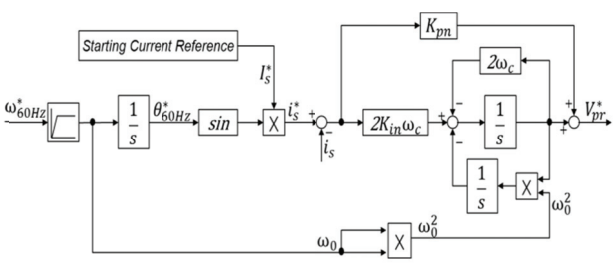

Fig. 6. Control block diagram of the proposed soft starting algorithm (during the starting operation region).

a PI controller, it is suitable for systems that have a starting time limit, such as compressors.

B. Mode Transition Algorithm Between Soft Starting and CVCF

An ultra-low temperature freezer basically runs at a constant speed which is 50 [Hz] or 60[Hz]. Therefore, the SPIM has to operate at constant voltage and constant frequency (CVCF) after the starting operation.

In the normal operation mode after start-up, if the target current is maintained by current control, even though a smaller current is required to operate SPIM, the current controller will be saturated. In other words, when the motor is already running, the PTC operates and operation current

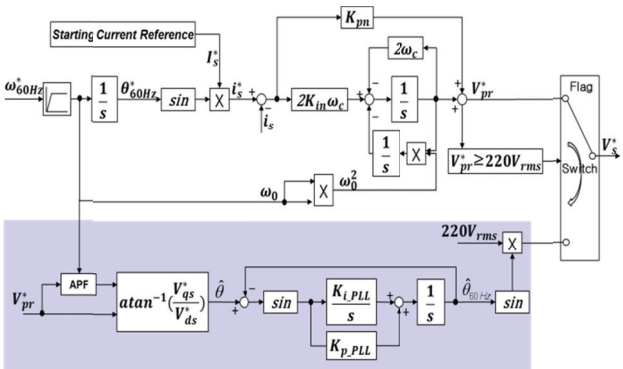

Fig. 7. Overall block diagram of the SPIM control system.

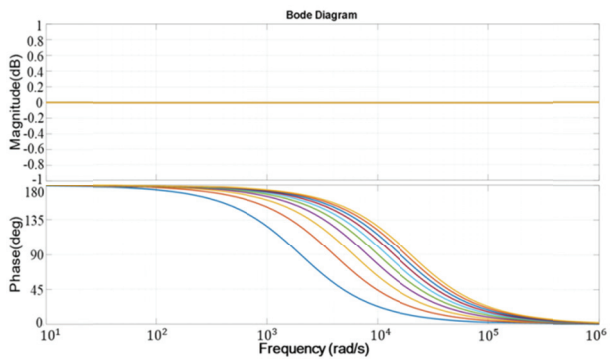

Fig. 8. Bode diagram of the all pass filter

becomes smaller than target current. Because of this, the current error becomes larger, which increases the control voltage and leads to inappropriate operation. That is the reason why the mode transition algorithm is necessary between soft starting and CVCF.

For mode transition, the voltage output and phase angle must be the same as the target voltage of the current controller. There are several methods such as zero-crossing detection, enhanced phase-locked loop and second-order generalized integrator to extract the phase angle of the source voltage [15]. In this paper, the arctangent based Phase Locked Loop (PLL) method is used to synchronize the phase angle with the voltage output of current controller [16]-[21]. Fig. 7 shows an overall block diagram of a SPIM including the soft starting control and mode transition control, respectively.

In order to generate a virtual voltage with a 90° phase shift from the source voltage, a low pass filter (LPF) or an all pass filter (APF) can be applied. While a LPF has a property that allows the magnitude and phase margin to change when the measured frequency is greater than the cutoff frequency, an APF has no a change in the magnitude margin as shown in Fig. 8 for all frequency ranges, thus only a phase margin is to be considered [20]. Therefore, an APF is used to generate the q-axis virtual voltage, v_{qs}^{*} with 90° phase difference from the output voltage of the current controller. The transfer function of the APF is expressed as:

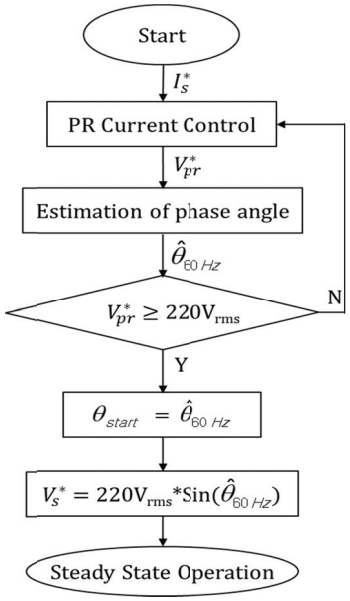

Fig. 9. Flow chart of soft starting and mode transition.

$$G_{APF}(S) = -\frac{s-\omega_A}{s+\omega_A} \tag{3}$$

where ω_A is the cutoff angular frequency.

As shown in Fig. 7, by using the generated arctangent value of equation (4), the phase angle can be estimated by using equation (5).

$$\hat{\theta} = a\tan^{-1}(\frac{V_{qs}^*}{V_{ds}^*}) \tag{4}$$

$$\hat{\theta}_{60Hz} = (\frac{K_{p\_PLL}s + K_{i\_PLL}}{s^2 + K_{p\_PLL}s + K_{i\_PLL}})\hat{\theta} \tag{5}$$

The mode transition is performed when the target voltage of the current controller reaches 220 V_{rms} as shown in Fig. 9.

IV. Experimental Results

There are tradeoffs that can be made to reduce the starting current in CSCR based SPIMs which is an unsymmetrical 2-phase system. If the current is too small, the torque is also small and motor is slow to start or the torque is actually too small to operate the motor. On the other hand, if the starting current is too large, the torque is large and motor is too quick to start, which can damage the system. Because of this, a suitable target current is determined according to the application.

Fig. 10 shows a photograph of the SPIM, which includes an ultra-low temperature freezer, power converter systems, and a control board. As shown in Fig. 11, the SPIM used in the experiments is based on the Capacitor-Start Capacitor-Run starting method. The full-bridge and 2 legs PWM inverter is implemented by IGBT modules with a switching frequency of 5 kHz.

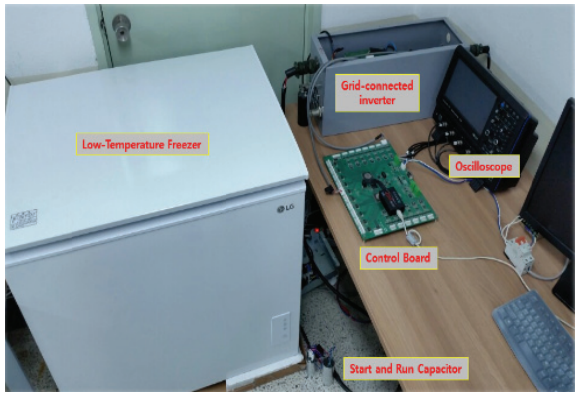

Fig. 10. Photograph of the experimental ultra-low temperature freezer using a SPIM driving system.

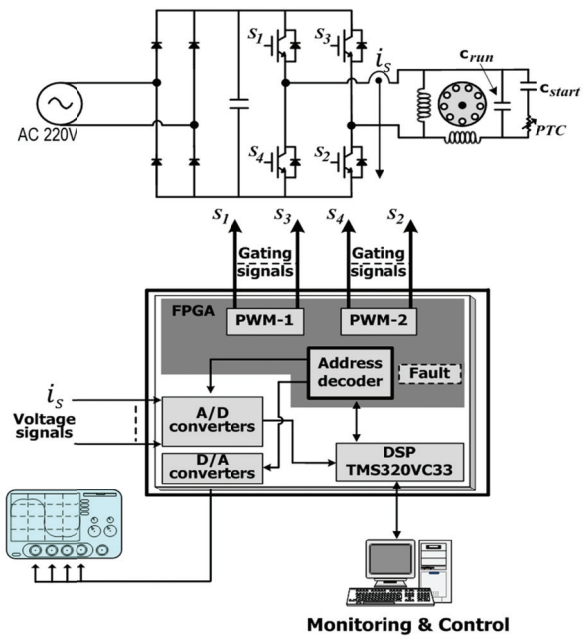

Fig. 11. Block diagram of a SPIM driving system using a 2-legs inverter.

TABLE II
Motor Specifications

Parameters	Value
Main Winding Resistance (ohm)	4.7
Aux. Winding Resistance (ohm)	21.97
Main Winding Inductance (ohm)	230
Aux. Winding Inductance (mH)	260
Running Capacitor [uF]	10
Starting Capacitor [uF]	75
Maximum Power [W]	1040
Rated Power [W]	260
Rated Torque [W]	3.1
Rated Speed [rpm]	3000
Number of Pole	2
Rated Frequency	60

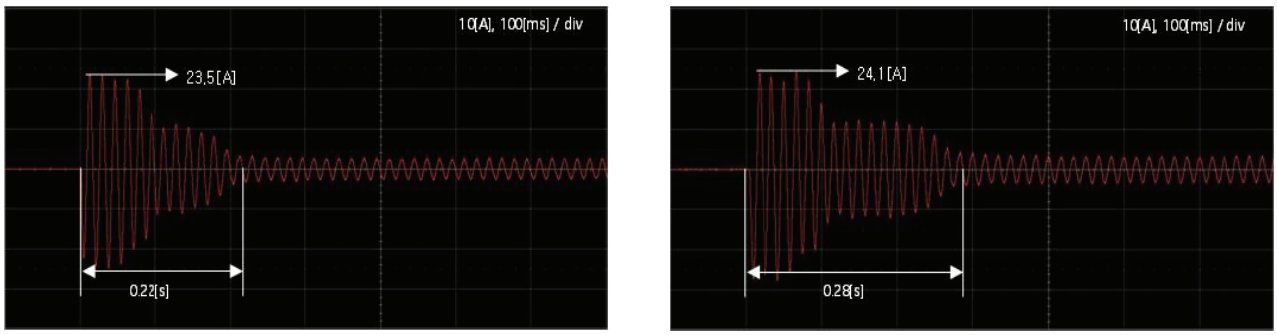

(a) (b)

Fig. 12. Experimental results of the direct starting of a SPIM: (a) Without soft starting (RT:-60°C); (b) Without soft starting (RT:-40°C).

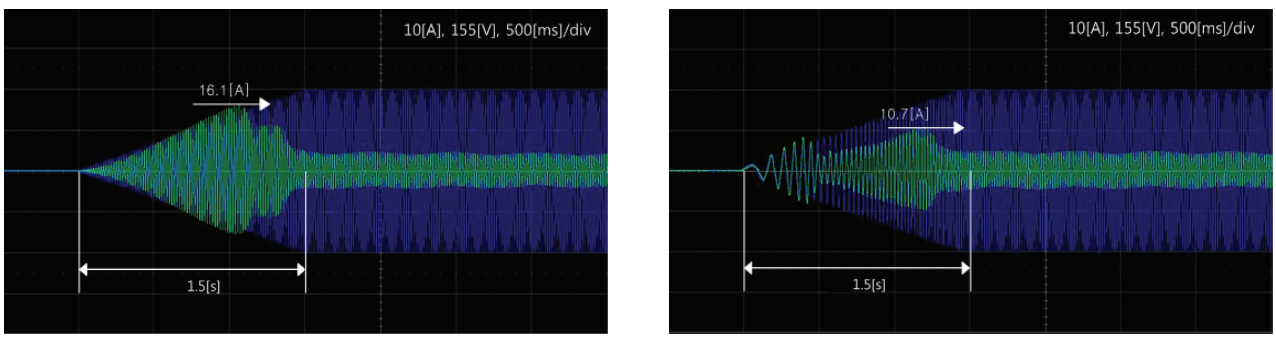

(a) (b)

Fig. 13. Experimental results of the voltage control of a SPIM: (a) With VVCF; (b) With VVVF.

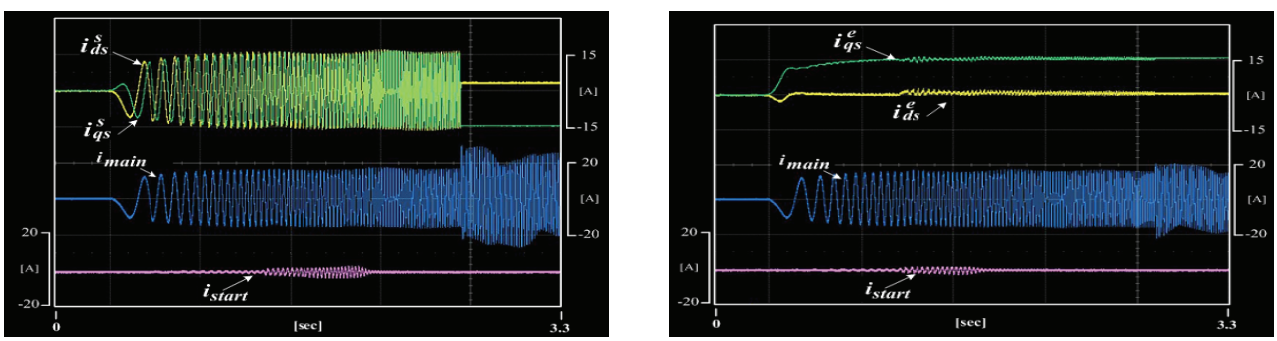

(a) (b)

Fig. 14. Experimental results of the PI current control in a SPIM (target current is 15A): (a) PI current controller at the stationary reference frame; (b) PI current controller at the synchronous reference frame.

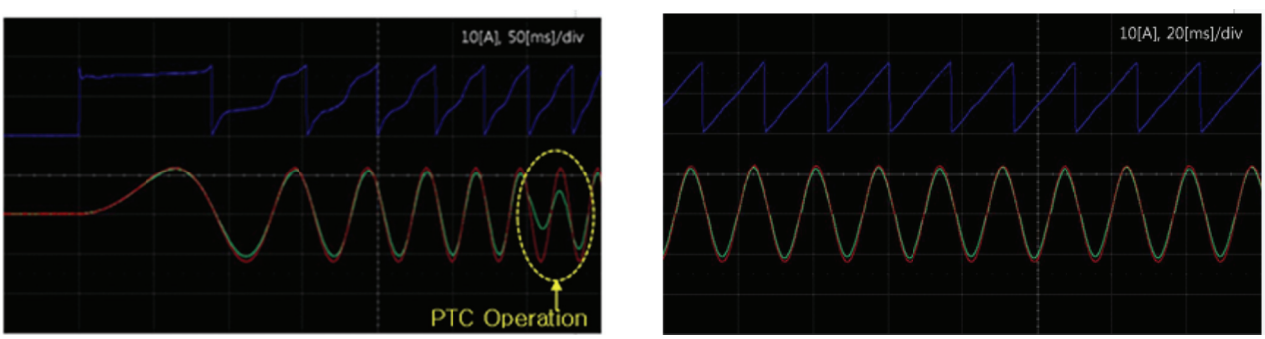

(a) (b)

Fig. 15. Phase angle generation for a mode transition (blue is for the estimated phase angle; red is for the current target; green is for the measured current): (a) Estimated phase angle during start-up; (b)Estimated phase angle before mode transition.

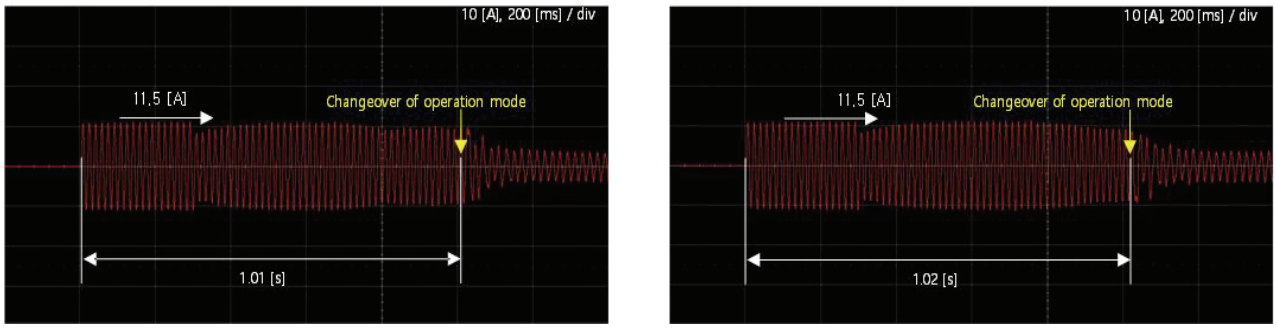

(a) (b)

Fig. 16. Experimental results of the PR current control in a SPIM(target current is 11.5A): (a) Soft starting by CFPR (RT:-60°C); (b) Soft starting by CFPR (RT:-40°C).

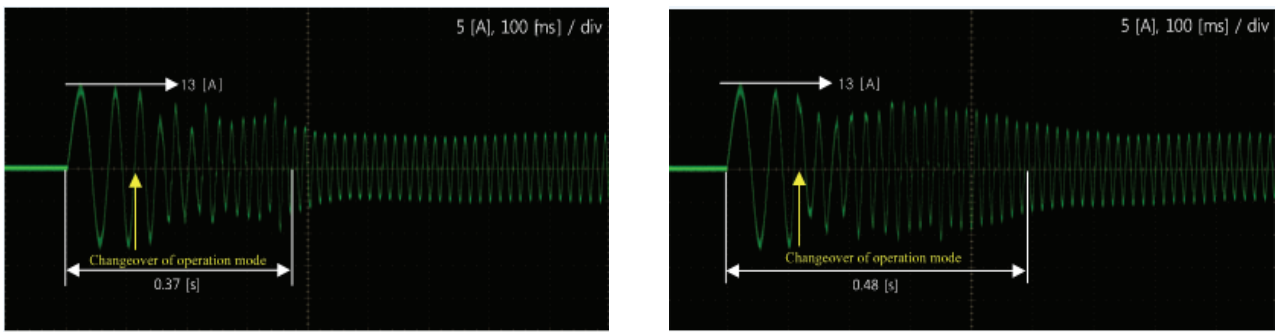

(a) (b)

Fig. 17. Experimental results of the PR current control in a SPIM (target current is 13A): (a) Soft starting by VFPR (RT:-60°C); (b) Soft starting by VFPR (RT:-40°C).

The specifications of the SPIM are presented as Table II. The control algorithm is performed by a digital signal processor (DSP) control system.

The starting methods of the SPIM used in the experiments consist of direct starting, voltage control which consists of VVCF and VVVF, and current control such as PI and PR.

In the direct starting scheme, the starting current is determined by a fixed circuit and it normally causes large current. Fig. 12 shows experimental results when the SPIM starts directly according to a variation in the room temperature from -60 [°C] to -40 [°C]. A high current of about 24 A can result in damage to the system.

The voltage control scheme consists of VVVF and VVCF. This method indirectly reduces starting current through voltage control. Fig. 13 shows the starting current of a SPIM when voltage control is applied. Even though VVVF can reduce the starting current to around 10A, the starting up time is still long. A long starting up time is not suitable for the application of a compressor.

Fig. 14 shows experimental results of a PI current controller with a target current of 15A. Fig. 14(a) shows results of a PI current controller with the stationary frame. It can be seen that the i_{qs}^{s} phase is delayed by 90 degrees from i_{ds}^{s}. Fig. 14(b) shows result of a PI current controller with the synchronous reference frame. It takes about 2.2 seconds start-up time, this because of the reference frame transformation/reverse transformation and obtaining the q-axis variable.

The proposed PR current control scheme consists of constant frequency proportional resonant (CFPR) and variable frequency proportional resonant (VFPR). The resonant frequency is constant at 60 Hz for the CFPR. However, it increases from 0 to 60 Hz for the VFPR during the start-up time. The generated phase angle for mode transition is shown in Fig. 15. The first part of the start-up time is shown in Fig. 15(a), and Fig. 15(b) shows the start-up time once it has been stabilized. The blue line represents the estimated phase angle, red is the target current and green is the measured current. Even though the measured current is reduced when compared to the reference current for 1 cycle because of the PTC operation in Fig. 15(a), the estimated phase angle is becoming smother and the measured current is fitting the reference current as time is going during the start-up. Fig. 16 and Fig. 17 demonstrate the starting currents of a SPIM when PR current controller and mode transition algorithms are applied with a variation of the room temperature from -60 [°C] to -40 [°C].

Experimental waveforms of the CFPR are shown in fig. 16 with a target current of 11.5A. The results of the VFPR are shown in Fig. 17 with a target current of 13 A.

Each algorithm tracks well with the starting current command and starting up time is reduced as well. It is shown

that the VFPR reduces the start-up time more than the CFPR.

V. CONCLUSIONS

This paper presents a new soft starting algorithm based on a PR current controller for an ultra-low temperature freezer. In addition, a mode transition algorithm is proposed to generate a constant voltage and a constant frequency (CVCF). A constant frequency proportional resonant (CFPR) and variable frequency proportional resonant (VFPR) current controller was proposed to reduce the starting current of a SPIM as well as the start-up time. In order to verify and realize the SPIM system, an ultra-low temperature freezer has been built with a 2-legs inverter controller.

The performance using PR current controller is compared with the direct start method, voltage control start and PI current controller. Experimental results show that the proposed method based on a PR current controller reduces both the starting current and the start-up time when compared to the direct start, voltage control start and PI current controller.

REFERENCES

[1] C. J. Kim, C. Y. Choi, D. E. Lee, G. S. Choi, and S. H. Baek, "Torque characteristics of single phase induction motor for phase control method," E*lectrical Machines and Systems, 2003 ICEMS*, pp. 510-513, Nov. 2003.

[2] E. Muljadi, Y. Zhao, T. H. Liu, and T. A. Lipo, "Adjustable ac capacitor for a single-phase induction motor," *IEEE Trans. Ind. Appl*., Vol. 29, No. 3, pp. 479-485, May/Jun. 1993.

[3] F. M. Bruce, R. J. Graefe, A. Lutz, and M. D. Panlener, "Reduced-voltage starting of squirrel-cage induction motors", *IEEE Trans. Ind. Appl*., Vol. 1A-20, No. 1, pp. 46-55, Jan./Feb. 1984.

[4] V. V. Sastry, M. R. Prasad, and T. V. Sivakumar, "Optimal soft starting of voltage-controller-fed IM drive based on voltage across thyristor," *IEEE Trans. Power Electron*., Vol. 12, No. 6, pp. 1041-1051, Nov. 1997.

[5] A. S. Ba-thunya, R. Khopkar, K. Wei, and H. A. Toliyat, "Single phase induction motor drives – A literature survey," *Electric Machines and Drives Conference, 2001 IEEE*, pp. 911-916, 2001.

[6] A. Khoei and S. Yuvarajan, "Steady state performance of a single phase induction motor fed by a direct ac-ac converter," *Proceedings of IEEE Conference,* pp. 128-132, 1989.

[7] D. Yildrim and M. Bilgic, "PWM AC chopper control of single-phase induction motor for variable-speed fan application," *34th Annual Conference of IEEE Industrial Electronics, 2008*, Vol. 1, No. 1, pp. 1337-1342, Nov. 2008.

[8] V. Thanyaphirak, V. Kinnares, and A. Kunakorn, "Soft starting control of single-phase induction motor using PWM ac chopper control technique," *Electrical Machines and Systems, 2013*, pp. 1996-1999, 2013.

[9] M. Caruso, V. Cecconi, A. O. Di Tommaso, and R. Rocha, "Sensorless variable speed single-phase induction motor drive system," *IEEE ICIT*, pp. 731-726, 2012.

[10] D. H. Jang and D. Y. Yoon, "Space-vector PWM technique for two-phase inverter-fed two-phase induction motors," *IEEE Trans. Ind. Appl*., Vol. 39, No. 2, Mar./Apr. 2003.

[11] D. N. Zmood, D. G. Holmes, and G. H. Bode, "Frequency-domain analysis of three-phase linear current regulators," *IEEE Trans. Ind. Appl*., Vol. 37, No. 2, pp. 601-610, Mar./Apr. 2001.

[12] N. Zhang, H. Tang, and C. Yao, "A sysmatic method for designing a PR controller and active damping of the LCL filter for single-phase grid-connected PV inverters," *Energies*, Vol. 7, No.6, pp. 3934-3954, Jun. 2014.

[13] F. O. Martinz, K. C. M. de Carvalho, N. R, N. Ama, W. Komatsu, and L. Matakas, "Optimized tuning method of stationary frame proportional resonant current controllers," in *Proc. IPEC 2014*, pp. 2988-2995, 2014.

[14] S. K. Sul, *Control of Electric Machine Drive Systems*, HongRung Publishing, pp. 224-228, 2016

[15] F. Blaabjerg, R. Teodorescu, M. Liserre, and A. V. Timbus, "Overview of control and grid synchronization for distributed power generation systems," *IEEE Trans. Ind. Electron*., Vol. 53, No. 5, pp. 1398-1409, Oct. 2006.

[16] G. Hsieh and J.C. Hung, "Phase-locked loop techniques. A survey," *IEEE Trans. Ind. Electron*., Vol. 43, No. 6, pp. 609-615, Dec. 1996.

[17] S. M. Silva, B. M. Lopes, B. J. C. Filho, R. P. Campana, and W. C. Boaventura, "Performance evaluation of PLL algorithms for single-phase grid-connected systems," *Conference Record of the 2004 IEEE Industry Applications Conference, 2004. 39th IAS Annual Meeting*, Vol. 4, pp. 2259-2263, 2004.

[18] M. Ciobotaru, "Reliable grid condition detection and control of single-phase distributed power generation system," Aalborg University, 2009.

[19] M. K. Ghartemani, "A unifying approach to single-phase synchronous reference frame PLLs," *IEEE Trans. Power Electron*., Vol. 28, No. 10, pp. 4550-4556, Oct. 2013.

[20] S. Golestan M. Monfared F. D. Freijedo, and J. M. Guerrero, "Performance improvement of a prefiltered synchronous-reference-frame PLL by using a PID-type loop filter," *IEEE Trans. Ind. Electron*., Vol. 61, No. 7, pp. 3469-3479, Jul. 2014.

[21] U. S. Seong, S. H. Hwang, "Analysis of phase error effects due to grid frequency variation of SRF-PLL based on APF," *J. Power Electron*., Vol. 16, No. 1, pp. 18-26, Jan. 2016.

Hae-Jin Kim was born in Sangju, Korea, in 1971. He received his B.S. and M.S. in Control and Instrumentation Engineering from Changwon National University, Changwon, Korea and Hanyang University, Seoul, Korea in 1994 and 1996, respectively. From 1996 to 2000, he was a Researcher at the Institute for Advanced Engineering(IAE), Yongin, Korea. Since 2000, he has been a Chief Engineer in the CAC Engineering Department, LG Electronics, Changwon, Korea. His current research interests include building management system, network protocol design and control of electrical machines. He is also a Registered Professional Engineer in the State of Texas, U.S.A.

Seon-Hwan Hwang was born in Korea. He received his B.S., M.S., and Ph.D. degrees in Electrical Engineering from Pusan National University, Busan, Korea, in 2004, 2006, and 2011, respectively. From 2011 to 2012, he was with the Center for Advanced Power Systems (CAPS), Florida State University, Tallahassee, FL, USA. In 2012, he joined the Department of Electrical Engineering, Kyungnam University, Changwon, Korea. His current research interests include the control of electrical machines, power electronics, and wind power generation systems.

Jang-Mok Kim was born in Busan, Korea, in 1961. He received his B.S. degree in Electrical Engineering from Pusan National University (PNU), Busan, Korea, in 1988; and his M.S. and Ph.D. degrees in Electrical Engineering from Seoul National University, Seoul, Korea, in 1991 and 1996, respectively. From 1997 to 2000, he was a Senior Research Engineer at the Korean Electric Power Research Institute (KEPRI), Korea. Since 2001, he has been with the School of Electrical Engineering, PNU, where he is presently working as a Faculty Member and as a Research Member in the Research Institute of Computer Information and Communication. As a Visiting Scholar, he joined the Center for Advanced Power Systems (CAPS), Florida State University, Tallahassee, FL, USA. His research interests include control of electric machines, electric-vehicle propulsion, and power quality.